Journal of Physics A: Mathematical and Theoretical



# Universal statistics of vortex tangle in three-dimensional random waves

To cite this article before publication: Alexander Taylor *et al* 2018 *J. Phys. A: Math. Theor.* in press https://doi.org/10.1088/1751-8121/aaa4ae

# Universal statistics of vortex tangle in three-dimensional random waves

**Alexander J Taylor**

H H Wills Physics Laboratory, University of Bristol, Tyndall Avenue, Bristol, BS8 1TL, UK

E-mail: alexander.taylor@bristol.ac.uk

**Abstract.** The tangled nodal lines (wave vortices) in random, three-dimensional wavefields are studied as an exemplar of a fractal loop soup. Their statistics are a three-dimensional counterpart to the characteristic random behaviour of nodal domains in quantum chaos, but in three-dimensions the filaments can wind around one another to give distinctly different large scale behaviours. By tracing numerically the structure of the vortices, their conformations are shown to follow recent analytical predictions for random vortex tangles with periodic boundaries, where the local disorder of the model 'averages out' to produce large scale power law scaling relations whose universality classes do not depend on the local physics. These results explain previous numerical measurements in terms of an explicit effect of the periodic boundaries, where the statistics of the vortices are strongly affected by the large scale connectedness of the system even at arbitrarily high energies. The statistics are investigated primarily for static (monochromatic) wavefields, but the analytical results are further shown to directly describe the reconnection statistics of vortices evolving in certain dynamic systems, or occurring during random perturbations of the static configuration.

## 1. Introduction

Many physical systems exhibit tangles of filamentary loops that wind around one another in a disordered fashion and resemble random walks on large scales. Examples are as diverse as $U(1)$ vortices on a random phase lattice introduced as early models for cosmic strings [1–3], the optical vortices of randomly scattered coherent light [4], closed 'worm' loops of alternating spin flavours in spin ices [5] or the Potts model [6], the molecular filaments of a polymer melt [7, 8], models of random spatial permutations [9], and the phase vortices in wave chaos that we investigate here [10, 11]. In many of these cases, the bulk *loop soup* of intertwining filaments appears to take on certain universal behaviours in large scale statistics such as the distribution of loop lengths. These results depend only on the isotropic random nature of the field and not on the specific local physics. The different behavioural regimes of ideal loop soups have recently been fully described by work on the universal statistics of vortex line tangles [12, 13], where the filaments display distinctly different types of behaviour at different lengthscales, depending on only a small number of parameters. The behaviour of short filaments below a physically-based correlation lengthscale is not universal and depends on the local physics of the system, but the tangle on larger scales approximates an ideal scale invariant loop soup with characteristic $-\frac{3}{2}$ power law in the frequency of loop lengths (this result matches earlier predictions from different arguments [1]). The model of [12, 13] further accounts for the effect of periodic boundaries, under which the global statistics

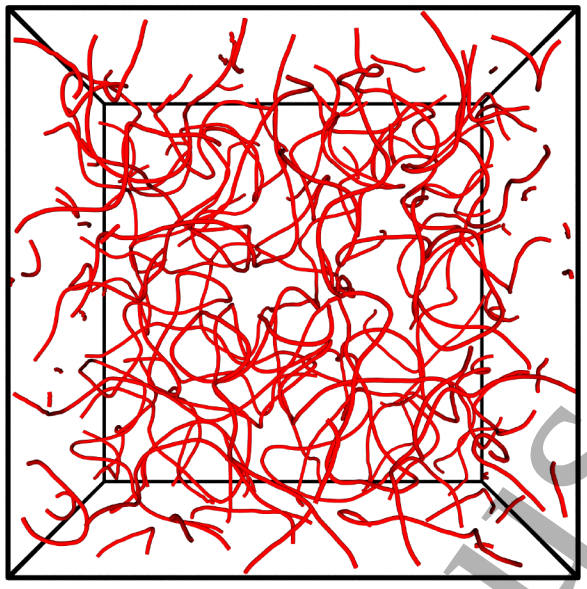

**Figure 1.** Tangled vortices in an example random wave with periodic boundaries. This model is introduced in Section 2, shown here with energy $E = 236\pi^2$ ($N^2 = 59$, see Section 2), periodic side length $3.84\lambda$. The tangle contains nine distinct vortices winding around one another.

of filaments much larger than the periodic side length are modified, the $-\frac{3}{2}$ power law is broken, and the filaments should take instead a Poisson-Dirichlet length distribution.

Here we study the tangle of *phase vortices* (nodal lines, phase singularities) in generic three-dimensional (3D) random wavefields, here arising from i.i.d Gaussian random weighted superpositions of randomly directed plane waves. These form a continuous exemplar of a fractal loop soup in which there is only one physical lengthscale, the wavelength [10, 14], and in which the random statistics of the field arise only from its initial conditions and not from extra physical processes. The vortices can be traced across all lengthscales from the smallest sub-wavelength structures whose geometry is dominated by the smoothness of the wavefield, to the largest scales of a given system [10, 14]. Despite the linear nature of the wave interference in which the randomness of the wavefield comes not from physical processes but only the initial conditions of the wavefunction, the vortex lines wind around one another to form complicated random structures, not morphologically dissimilar to those in far more complex physical systems [10, 15].

We use the *random wave model* [16], where the wavefield $\psi$ is given by a superposition of plane waves:

$$\psi(\boldsymbol{r}) = \sum_n a_n \exp(i(\boldsymbol{k}_n \cdot \boldsymbol{r} + \chi_n)) \ , \tag{1}$$

for i.i.d Gaussian random complex $a_n$, uniform random phase $\chi_n$, and randomly oriented $\boldsymbol{k}_n$. The sum over $n$ is in principle infinite, but in practice the statistics of the wavefield converge rapidly as $n$ grows larger than a few tens. This can model for many types of random physical system; in particular, when $|\boldsymbol{k}_n| = k$ the random wave model is an excellent statistical model for high energy eigenfunctions of the Laplacian, $\nabla^2\psi = -E\psi$, well established in two-dimensional ergodic cavities far from the boundaries [16]. However, (1) is not restricted to two dimensions or even to the monochromatic spectrum, and can be a statistical model for many different kinds of disordered

wavefields such as random interference in acoustic resonances [17] or optical volume speckle [4, 18], as well as 3D resonances of chaotic cavities directly analogous to 2D quantum chaos. Phase vortices occur generically in these types of wavefield; they are nodes (zeros) of the amplitude, and the complex phase circulates by $2\pi$ in any path around the vortex core (in principle $2n\pi$ for any integer $n$, but higher values generically do not occur). Figure 1 shows a typical example of such vortex paths, numerically traced in a 3-torus eigenfunction with energy $E = 236\pi^2$; this modified random wave system is described in Section 2. While eigenfunctions of this type could be written in terms of real wavefunctions, complex waves could be used to represent e.g. the breaking of time-reversal symmetry in cavities with lossy boundaries (represented via imaginary reflection coefficients). Here we do not model such effects directly, and choose waves of this form primarily to access the loop soup phenomena.

The random wave model has received particular interest as a statistical model for chaotic eigenfunctions in two dimensions, in which case the eigenfunctions are time-reversal symmetric and so generally taken to be real (equivalent to taking the real or imaginary component of (1), as these are independent). The nodal filaments are then a core structure whose varied conformations capture the chaotic character of the wavefunction [19]. Although they are confined to the plane and so cannot truly be tangled around one another, the nodes form complicated extended conformations across all lengthscales, bounding extended nodal domains of all-positive or all-negative value. The local shapes of the random structures are heavily influenced by the fact that they generically do not intersect [20], but they do have a scale-invariant random character on larger scales [21]. Considering the nodal domains as equivalent to the connected clusters in models of bond [22] or site [23, 24] percolation, certain nodal domain statistics including their density, distribution of areas and fractalities have been shown to strongly reproduce the predictions of the percolation models.

Much of the analysis of vortex filaments in 3D complex random waves has focused on the counterparts of these statistics that are well understood in two dimensions. Certain statistical quantities, including the density of vortex lines per unit volume and probability distribution of vortex curvatures, have been computed analytically [15]. However, other large scale quantities such as the fractality of the vortices [4, 10] (both individually and in bulk), and the distribution of their lengths [10, 11], have been directly computed only numerically. These simulations generally take place under periodic boundary conditions in order to be able to follow individual vortex lines across large lengthscales [4, 10], which also allows for a numerical analysis of tangling in terms of the vortex topologies, as they may knot or link with one another [14, 25]. The measurements have confirmed that the vortices of these random tangles appear to have Brownian random character resembling random walks at all lengths beyond some small correlation lengthscale [4, 10]. On large scales, the loop frequencies appear to follow a power law scaling relation with respect to the loop lengths [10, 11], consistent with predictions for an ideal loop soup with no boundaries, as previously observed in other vortex models [1, 10].

It is natural to expect that these three-dimensional scaling laws may also have deep relations with models from statistical physics. However, it has been unclear what governs these results, as the analytical machinery to compare nodal lines with models from statistical physics is less well developed in three dimensions. Certain features of the wavefield have also appeared inconsistent

with the behaviour of an ideal loop soup; extremely long vortex lines occur far more frequently than the power law would indicate, usually wrapping around the periodic boundaries a non-zero total number of times before returning to their starting point [1, 10]. These wrapping lines have *non-trivial homology* (NTH), and would appear as infinite (periodically repeating) lines in a tiling of space with the periodic cell, but infinite lines are not compatible with the loop length distribution in an ideal infinite loop soup [1]. To contrast with this behaviour, we sometimes refer to lines with trivial homology as 'closed loops', indicating that they do not ultimately 'wrap around' any periodic direction before closing. The NTH lines appear to be a manifestation of similar phenomena in certain lattice models [1], which can in these cases be understood as a percolation phenomenon; the bond percolation threshold on these lattices is always lower than the vortex connectivity enforced by the model, so some fraction of vortex length is guaranteed to appear in lattice-spanning 'infinite' lines [3]. However, this result relies on the lattice structure, whereas the vortices of the random model appear in a continuous field. It is natural to expect that the NTH lines might result from a finite-size effect coming from the periodic boundaries, but their frequency of occurrence has not appeared strongly related to the periodic side length [11].

We show here that the scaling relations of vortex loop soups, across all regimes from the wavelength scale to the large lengths where NTH lines dominate, are predicted by recent work on the universal statistics of vortex line tangle in short range correlated fields [9, 12, 13]. Following [13], the periodic boundaries change the statistics of how vortices approach one another even at arbitrartily high energies, introducing an extra scaling regime for lines long enough to explore the whole periodic cell. In Section 2 we show that the predictions of this model accurately quantify the statistics of length distribution in random wave vortices. These results are demonstrated numerically via large scale simulations of vortex tangle, in which the vortices are accurately tracked across all lengthscales to reconstruct the geometry of every filament. In Section 3 we use extensions to the numerical model to follow vortex curves as they reconnect with one another under different types of time evolution, and show that the statistics of reconnection frequencies between vortices of different lengths are strongly affected by the periodic boundaries. These effects are well described by the predictions of [13], and we demonstrate that reconnection processes directly reproduce an ideal statistical split-merge description of vortex line dynamics [12].

## 2. Loop soup statistics of vortex tangle

Although the random wave model (1) is an ideal model for unbiased random wavefields, it is difficult to numerically track the vortex loops across many different scales. Within any numerically sampled volume only a relatively small number of vortices will form closed loops, while others appear as vortex segments that terminate on the volume boundary. In accordance with the literature [4, 10], we resolve this issue by introducing periodic boundaries so that individual vortices can be followed along their entire lengths rather than terminating on the edges of the sampled cell, even if they wrap around them before closing and so form NTH lines. Some previous work enforces a finite volume tangle by instead working with degenerate eigenfunctions of different manifolds, such as the 3-sphere or three-dimensional harmonic oscillator, but these are less numerically tractable, and certain statistics vortex tangle appear strongly affected by the boundary conditions even at relatively high energies [14]. We impose periodicity $\psi(\boldsymbol{r}) = \psi(\boldsymbol{r} + l\boldsymbol{X} + m\boldsymbol{Y} + n\boldsymbol{Z})$, for any integers

$l, m, n$ and orthogonal vectors $\boldsymbol{X}, \boldsymbol{Y}, \boldsymbol{Z}$ with $|\boldsymbol{X}| = |\boldsymbol{Y}| = |\boldsymbol{Z}|$ (i.e. a cubic cell). To meet this condition the random wave model (1) must be modified to allow only wavevectors compatible with the fixed side length of the periodic unit cell, i.e. of the form $\boldsymbol{k}_n = \frac{2\pi}{|\boldsymbol{X}|}(p, q, r)$ for dimensionless integers $p, q, r$. The eigenvalue is then $E = 4\pi^2 N^2/|\boldsymbol{X}|^2$ with $N^2 = p^2 + q^2 + r^2$. Since we study eigenfunctions the spectrum is monochromatic, $|\boldsymbol{k}_n| = k = \sqrt{E}$. The characteristic lengthscale is the wavelength $\lambda = 2\pi/k$, and the valid wavevectors correspond to the intersections between a sphere of radius $N$ with integer valued lattice points.

Although our use of periodic boundary conditions is intended to approximate the isotropic random wave model, they equivalently define random waves on the 3-torus, which have been studied in the literature as *arithmetic random waves* [26] (referring to the arithmetic condition on valid wavevectors). However, the statistics then depend strongly on the number and distribution of valid wavevectors at a given $N$ (i.e. the degeneracy of the eigenfunction), which will not be isotropically distributed on the direction sphere [26, 27], especially when $N$ is small. The degeneracy also varies significantly even when $N$ is large, for instance it can often be zero even at energies far greater than investigated here. This poses a numerical problem, as the periodic boundaries cannot be expected to be anything like a good approximation of the isotropic model unless the energy is chosen to allow a large number of relatively evenly distributed wavectors, but at very high energies the numerical cell needed for vortex resolution becomes impractically large. However, previous work has established that in fact arithmetic random waves with relatively low $N$ can reproduce many statistics of the isotropic random wave model [4, 10], including fractal scalings similar to those we investigate here.

The following results come from large scale simulations of the loop soups in arithmetic random waves at each of $N^2 = 59$, $N^2 = 243$ and $N^2 = 675$, whose degeneracies are 36, 52 and 112 respectively. The cases of $N^2 = 243$ and $N^2 = 675$ match those in [10] while the smallest energy, $N^2 = 59$, is chosen because of the relatively small total vortex length within such a small cell, allowing the vortices to be tracked and analysed relatively rapidly in the cases where statistics can only be generated from many iterated simulations. Although these degeneracies are not especially high, they are all selected as local degeneracy maxima while also possessing the additional symmetry $\psi(\boldsymbol{r} + l|\boldsymbol{X}|/2 + m|\boldsymbol{Y}|/2 + n|\boldsymbol{Z}|/2) = (-1)^{l+m+n}\psi(\boldsymbol{r})$, implying that the nodal lines in each octant of the periodic cell are identical (although the local signs of the real and imaginary field components may be different). Some nearby energies have a slightly higher degeneracy but lack the octant symmetry; this is more general but the unit cell of the vortex pattern becomes instead a truncated octahedron, whose periodicities are more difficult to implement numerically and so are not preferred here. In the following analysis, we choose as our unit cell a single unique octant of each eigenfunction, such that the nodal lines have no additional symmetry (the same methodology was used in [10, 11]). The side length $|\boldsymbol{X}|/2$ of the toroidal octant can be expressed as $L\lambda$ where $L = N/2$, and is therefore approximately $3.84\lambda$, $7.79\lambda$ and $13.0\lambda$ at each of $N^2 = 59, 243, 675$.

The vortices forming the loop soup are numerically located and tracked using their local phase structure. The $2\pi$ circulation of the complex phase can be detected by any phase integral around the vortex core, even arbitrarily far from it, as long as no other vortices are contained within the integral region. The full tangled vortex structure is accurately reconstructed via the recursively resampling Cartesian grid algorithm introduced in [10, 11]. This first approximates

the vortex positions using numerical integration around the plaquettes of a Cartesian lattice with relatively low resolution. If vortex path is not traced unambiguously, the problematic local regions of the lattice are then resampled at a progressively higher resolution until the full vortex loop is found. This corrects two primary tracing errors: a naive numerical integration might not always detect the passage of the vortex (so the loop appears broken); and vortices regularly approach closely on the lattice scale during near-reconnections, so that multiple vortices enter the same numerical lattice cell and their connectivity cannot immediately be resolved. In both cases, phase integration at a sufficiently high resampled resolution will eventually locate the paths of the vortices, regardless of the surrounding wavefield. The base numerical resolutions for the recovered vortex line representations are $\sim 0.035\lambda$ at $N^2 = 59$ and $\sim 0.09\lambda$ at $N^2 = 243$ and $N^2 = 675$, with the higher resolution at $N^2 = 59$ chosen to enhance the resolution of reconnection events in the later analysis, although even the lower resolution is well below the vortex correlation lengthscales (geometrical decorrelation occurs on the scale of $\sim \lambda$ [10]). Since the local resolution is increased by the algorithm where necessary to unambiguously capture the vortex path, these values are minimum sampling resolutions for the recovered vortex curves. Changing the initial resolution does slightly affect the measured lengths of the recovered curves, but this error is small compared to the other quantities considered below (on the order of 0.5% if the resolutions here are halved or doubled), and should be especially unimportant when considering quantities expressed as length fractions. With these parameters, tracking the vortices in a single random wave with $N^2 = 59$ takes $\sim 140s$ on a modern laptop, while an $N^2 = 243$ eigenfunction takes $\sim 80$s [10] and an $N^2 = 675$ eigenfunction takes $\sim 360$s [11].

The higher energy eigenfunctions $N^2 = 243$ and $N^2 = 675$, analysed by these methods, have previously been established to closely reproduce certain local statistics (densities, curvatures, fractalities [10]) of the isotropic random wave model, and on large scales the the closed loops (but not NTH lines) have the length distribution of a loop soup [10, 11]. In order to confirm that the numerical errors in recovering our vortex tangle are comparable with these previous results, the same density comparisons are as follows for eigenfunctions at $N^2 = 59$ (at $N^2 = 243$ and $N^2 = 675$ the numerical parameters exactly match those of [10]): the average density of nodal lines through an axis-aligned plane is $(2.11 \pm 0.04)\lambda^{-2}$, compared to the expected value of $2\pi/3\lambda^2 \approx 2.09\lambda^{-2}$ in the isotropic model [15], while the volume density is $(4.59 \pm 0.02)\lambda^{-2}$ compared to the isotropic value $4\pi/3\lambda^2 \approx 4.19\lambda^{-2}$ [15]. The planar density matches the theoretical expectation well, while the volume density is $\sim 10\%$ higher. A comparable discrepancy was also seen in [10] even at higher energies, and was thought there to arise from the torus periodicity encouraging vortex loops. Following these previous results, we anticipate that these discrepancies should not significantly affect most statistics, but an error on the order of up to $\sim 10\%$ cannot be excluded from other numerically recovered quantities. Since these results are no worse than at $N^2 = 243$ or $N^2 = 675$ (or even $N^2 = 1875$ [10]), we anticipate that in fact the large scale results below are quite robust to finite size effects beyond the immediate discrepancy in the numerically recovered value.

A core scaling feature in ideal loop soups is that the filamentary tangle should be scale invariant across all lengthscales beyond some small-scale cutoff. The cutoff arises here from the smoothness of the wavefield at the wavelength scale or lower, but in other situations could arise from e.g. the lattice spacing in discrete models. This fractality requires a particular power law in the scaling of

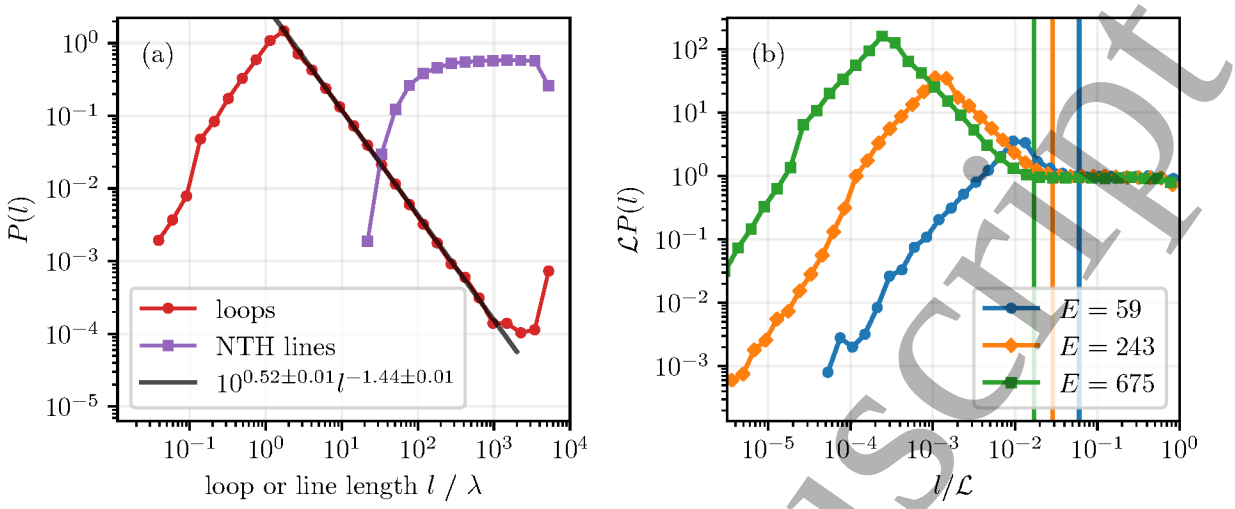


**Figure 2.** Probability distributions by length for loops and NTH lines in random waves with periodic boundaries. (a) shows on a log-log scale the probability distributions of vortex lengths for each of the 2583322 closed loops (green) and 37745 NTH lines (purple), normalised separately, taken from 9500 different numerically-recovered random waves at $N^2 = 675$. The black line shows a least squares fit to the apparent power law between $l \approx 10^{0.5}$ and $l \approx 10^3$, given by $P(l) = 10^{0.52\pm0.01}l^{-1.44\pm0.01}$. (b) shows on a log-log scale the combined probability distributions of vortex lengths for both loops and NTH lines, for random waves with periodic boundaries at three different energies $N^2 = 59$ (63114 vortices from 7157 random wave simulations), $N^2 = 243$ (1278186 vortices from 19845 random wave simulations) and $N^2 = 675$ (2621067 vortices from 9500 random wave simulations, the same dataset used in (a)). Each vortex arclength is normalised by the total vortex arclength in its random wave. The peak in each case corresponds to $\sim 3.5\lambda$. The vertical lines mark the lengthscale $L^2\lambda$ at each energy, where $L\lambda$ is the side length of the periodic cell, and correspond to the expected crossover from an ideal loop soup power law to a Poisson-Dirichlet distribution.

loop lengths, with the number of loops of length $l$ decaying as $l^{-\frac{3}{2}}$. The exponent arises from the combination of Brownian fractality of the individual vortices and the requirement that geometry of the tangle cannot depend on the scale (a full derivation is given in [1, 2]), or equivalently can be obtained as the probability distribution for the lengths of random walks in three dimensions that are conditioned to return to their origin [7]. This power law is therefore to be expected from the numerical simulations described above, and has been found previously to hold for the closed loops in the same arithmetic random wave model [4, 10], at lengthscales between $\sim 3.5\lambda$ (below which local correlations dominate) up to almost the very largest loop scales. However, this counts only the loops with trivial homology, and the NTH lines present in all of these numerical experiments have not appeared consistent with this scaling law.

Figure 2(a) shows this scaling regime as expressed in arithmetic random waves with $N^2 = 675$. The loops exhibit a power law scaling with gradient $-1.44 \pm 0.01$ across almost three orders of magnitude, consistent with previous results in the same model [10], and with the discrepancy from the anticipated $-3/2$ thought to arise from the finite volume of the system. The distinctly different scaling of lines with non-trivial homology is also shown, and these lines occur across all lengthscales larger than the cell side length (the shortest possible length for a NTH line). As

expected [10] the NTH lines do not appear to follow a power law in their length distribution, despite their local geometrical similarity to closed loops, and the fact that their wrapping number around the boundaries is generally small compared to their total length. At lengthscales beyond the cell side length they rapidly become much more numerous than closed loops, but even in this regime the closed loops continue to follow the loop soup power law across at least one further order of magnitude, although this eventually breaks down and the loops increase in frequency again at length fraction $\sim 1$. These longest loops often consume over half the the arclength in the periodic cell. This final peak appears to arise from the fact that there must always be either 0 or at least 2 NTH lines in order for their wrapping numbers vectors to add to 0, as by continuity the periodic cell cannot accumulate phase circulation on its boundary. The peak in loop probability appears to correspond to loops so long that the system does not contain enough 'spare' vortex arclength for an NTH line with opposite wrapping to be likely to exist, so the relative likelihood of extremely long loops compensates for missing NTH lines to preserve their own, otherwise-flat distribution. It is natural to expect that the presence of NTH lines and their coupling to the loop distribution may jointly be corrections to the scaling due to the periodic 'confinement' of the box, but previous analysis has found no clear dependency on the energy of the eigenfunction [11].

The universal vortex statistics introduced in [12, 13] provide a unified perspective on the behaviour of both closed loop and NTH line vortices [12]. Following [13], the distribution of vortex loop lengths under periodic boundary conditions has a more complex form that incorporates but is not fully described by the power law of an ideal loop soup, with the vortices of length $l$ falling into three distinct regimes. At low energies below a correlation length $\xi$, the loop statistics depend on the system, here being limited ultimately by the smoothness of the field on the scale of the wavelength. At scales $\xi \ll l \ll L^2\lambda$ the loops are Brownian which implies a $-d/2$ power law for loop length scaling in $d$ dimensions, consistent at $d = 3$ with the ideal loop soup model of [1]. This regime represents those lines that are large enough not to be dominated by local correlations but small enough not to wind through a local volume larger than the periodic cell, such that they do not 'feel' its boundaries. The scaling with $L^2\lambda$ arises from the fact that the vortices, as random walks, have fractal dimension 2. In general, these loops are not large enough to wrap around the boundaries and approach periodic 'copies' of themselves. Although this regime can be clearly observed in Figure 2 below the $L^2\lambda$ lengthscale, the $-3/2$ power law continues in Figure 2(a) for loops up to at least 50 times longer.

Finally, at scales $l \gg L^2\lambda$, the combined distribution of loop and NTH line lengths is expected to be Poisson-Dirichlet (PD) [13]. It should have the form

$$P(l) = \frac{\theta}{\mathcal{L}}\left(\frac{1-l}{f\mathcal{L}}\right)^{\theta-1} , \tag{2}$$

where $\mathcal{L}$ is the total loop length in the system (here $\mathcal{L} = 4\pi L^3\lambda/3$ [15]) and $\theta$ depends on certain properties of the loop system, whether the loops are oriented, and a *fugacity* $f$. If the loops are oriented then $\theta = f$, otherwise $\theta = f/2$ [13]. The fugacity is a real positive parameter that affects how the loops equilibrate through reconnections [12, 29]. If $f$ is an integer, it can be interpreted as giving each loop one of $f$ different colours; a soup with $\mathcal{C}$ loops can have $f^{\mathcal{C}}$ different configurations. In direct numerical models of loop soups only loops with the same colour may reconnect during loop equilibration, although random recolouration is also a part of the algorithm and the loop soup

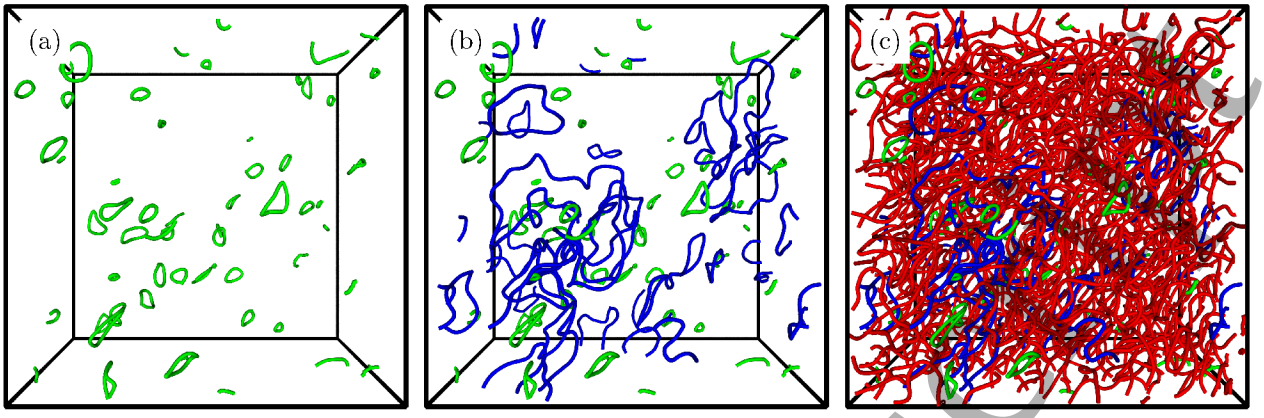


**Figure 3.** Vortices across different lengthscales in a 3-torus eigenfunction with $N^2 = 243$ (side length $3.78\lambda$). (a) shows in green only the short vortices below the scaling cutoff $\xi \approx 3.5\lambda$, which form perturbed ellipses [28]. (b) adds in blue the vortices in the regime $\xi < l < L^2\lambda$, i.e. large enough to take random conformations but smaller than the scale of the torus sidelength. (c) adds the vortices in the final length regime $l > L^2\lambda$, shown in red. The short vortices in the green and blue regimes are most numerous, but the majority of total vortex arclength is contained within a small number of long vortices with $l \gg L^2\lambda$.

statistics are recovered only as an average over all colourations [29]. Although these parameters can describe a broad class of loop soups, the vortices in random wavefields are oriented by their direction of local phase rotation but have fugacity 1 [12] (there are no extra correlations in their reconnections), so $f = \theta = 1$ and (2) simplifies to $\mathcal{L}^{-1}$.

Figure 3 shows how these regimes are expressed in vortex loop soups via an example at $N^2 = 243$. (a) includes only the short loops in the regime $l < \xi$, where the loops are not large enough to behave as random walks and form instead perturbed ellipses [28]. (b) adds the loops in the $-3/2$ fractal scaling regime, where the loops are large enough to behave randomly, but not so large that they can fill the periodic cell. (c) finally adds the longest lines, which are relatively few in number but often consume most of the total arclength in the cell and usually have non-trivial homology (in the Figure, every vortex in this regime has NTH).

Figure 2(b) shows the combined loop/NTH linelength PDF for vortices at each of the investigated energies $N^2 = 59, 243, 675$. In each case all three regimes can be clearly distinguished. The crossover between small- and large-scale behaviour occurs at $\xi \approx 3.5\lambda$, consistent at all energies and with previous measurements [10]. The position of the later crossover to the Poisson-Dirichlet regime scales with $L^2\lambda$, as anticipated, marked here for each energy by a vertical line, although this only approximately locates the crossover as the transition between regimes is not perfectly sharp. The PDF is flat beyond this point and $P(l) \propto \mathcal{L}^{-1}$, even at relatively low degeneracies.

These results make it clear that the NTH lines arise from the periodic 'confinement', with their statistics depending directly on the lengthscale at which a vortex line becomes long enough to 'feel' itself through the periodic boundaries. However, when $L$ grows arbitrarily large, there will always be a small number of increasingly long vortices in the Poisson-Dirichlet regime, even as the volume of the periodic cell and number of closed loops in the fractal regime grow rapidly. In fact the contributions of lines in the Poisson-Dirichlet regime, which will usually have non-trivial homology, rise at the same rate as the length contribution from closed loops with $P(l) \propto l^{-3/2}$ [13].

According to these relative frequencies, when $L$ is large the vortex arclength in closed loops makes up on average $\sim 25\%$ of the total vortex length in a given cell, although this result assumes a sharp transition between the two regimes and that the closed loops follow a $-3/2$ power law even in the Poisson-Dirichlet regime. It also does not count the vortex length in the small loops with $l < 3.5\lambda$, whose frequencies are not described by the ideal model. However, as local phenomena their frequency depends primarily on $L^3$, and in practice small loops appear to contribute less than half as much vortex arclength as the closed loops in the fractal regime. Accounting for all these approximations, we anticipate that the closed loops in periodic random wave vortex tangle with high $L$ will make up no more than 40% of the total arclength on average, with the rest of the arclength always expressed in a relatively small number of lines with NTH. This loop length fraction is much higher than the 20% seen in practice [4, 10], but these previous numerical results all consider a relatively small $L$ in which the vortices do not yet approach an ideal configuration. In particular, we noted in Figure 2(a) that our power law fit has gradient $-1.44 \pm 0.01$ compared to the ideal $-3/2$, with the difference attributed to the finite system size. Although this does not appear to affect our main results, it does significantly reduce the fraction of vortex length in this regime.

## 3. Vortex reconnections in dynamic systems

The different statistical regimes discussed in Section 2 are properties of the static vortex tangle. In our wavefields the vortices have no physical dynamics and their random statistics arise only from the random parameters of (1). However, the same result should arise from time evolution in appropriate random systems. For instance, even in linear isotropic wave superpositions that are not monochromatic (i.e. the wavevectors have some spectrum in $k$), or fields with time-varying phase (i.e. random waves $\exp(i(\boldsymbol{k}\cdot\boldsymbol{r} + \omega t + \chi))$ for some frequency $\omega$), the vortices are no longer static but will move around [15]. They may sometimes change their local topology by *reconnecting* with one another, or shrink to nothing as small loops, or likewise appear from nothing [28]. As long as the wavefield remains a loop soup, the distribution of vortex arclength must be a statistical steady state under these processes.

The Poisson-Dirichlet regime can itself be understood statistically as the result of a split-merge process between the different nodal lines, in which individual vortex lines reconnect randomly such that the limiting distribution of their lengths is (2) [9, 13]. The steps of this split-merge procedure are [9]:

- Choose a first vortex line $i_1$ with probability proportional to its length $l_1$.
- Independently choose a second vortex line $i_2$ with probability proportional its length $l_2$ (this may be the same line).
- If $i_1$ and $i_2$ are the same line, split the line to form two shorter lines with lengths $ul$, $(1-u)l$, for $u$ uniform random in [0, 1].
- If $i_1$ and $i_2$ are different lines, join them to form a single longer line of length $l_1 + l_2$.

The Poisson-Dirichlet distribution is recovered in the limit of repeated applications of this procedure. In physical systems the role of the periodic boundaries is that they allow for long

vortices to roam throughout the box without being strongly locally biased. These long lines in the Poisson-Dirichlet regime tend to approach every point in the box, including passing close to all other regions of themselves. Under random reconnections the resulting statistics are therefore perturbed from the ideal loop soup power law despite the local uniformity of the cell.

The local shape of vortices during reconnections depends only on the local geometry of the wavefunction [28]. Since the wavefield decorrelates on approximately the scale of the wavelength $\lambda$, we expect that reconnections should mostly be independent random events. We investigate here whether they in fact replicate the split-merge process of the Poisson-Dirichlet distribution; it would then describe not just an algorithm to reproduce the statistical distribution of vortex lengths, but the actual large scale behaviour of vortex tangle in random wavefields, even in systems with e.g. very different spectra. Since these statistics are universal to random vortex tangles, the same model should even describe the local structure of configuration space for monochromatic waves; perturbations to random wave parameters that preserve their random statistical distributions will likewise cause vortices to move and reconnect, with the same relative probabilities.

We investigate this reconnection behaviour numerically, via extensions to the monochromatic random wave eigenfunctions previously introduced. The reconnections can be detected by observing how the distribution of the vortex lengths changes during perturbations to the wavefield. For any given configuration, the RRCG algorithm (Section 2) can retrieve the number of vortices in the wavefield, and the length of each one. If the wavefield is perturbed, the same procedure can be repeated and in general the lengths of the vortices evolve smoothly while the number of vortices does not change. The exceptions to this are during reconnections, or the birth and death of small loops as they appear from (or shrink to) nothing [28]. Reconnections are seen as an instantaneous jump in the length distribution where one vortex splits into two components (or two vortices join together) and the total number of different vortices increases (decreases) by one. The exact vortices involved in the reconnection can be isolated by checking for a long vortex with a length close to the sum of two now-missing vortex lengths on the other side of the reconnection. Detecting reconnections in this way often works even when multiple reconnections occur in a single numerical step, as long as the changes in length of individual vortices can be distinguished from the incremental changes of evolution without reconnection. These techniques can also detect the birth or death of small loops; a birth (death) is recorded when the number of vortices in the wavefield increases (decreases) by one, but the only change in length distribution is the appearance (disappearance) of a very short loop.

In practice, at accessible numerical resolutions almost all reconnections can be distinguished from normal loop evolution in the length spectrum. Reconnections involving the smallest loops may be missed, but these are rare, and not important to the loop-soup description of reconnection rates as this applies only to long vortices in the Poisson-Dirichlet regime. It would also be possible to further numerically isolate the vortices involved in the reconnection, and to find the exact spatial position of the event, but we do not do so below as it is not necessary for the recovery of reconnection statistics. The numerical detection of loop births and deaths should also capture the real behaviour of the tangle; although the disappearance of a loop does not guarantee that it has actually shrunk to nothing, only that it has shrunk below the lengthscale of the lattice, our initial numerical lattice has side length $0.035\lambda$ which is well below the wavelength scale at which loops

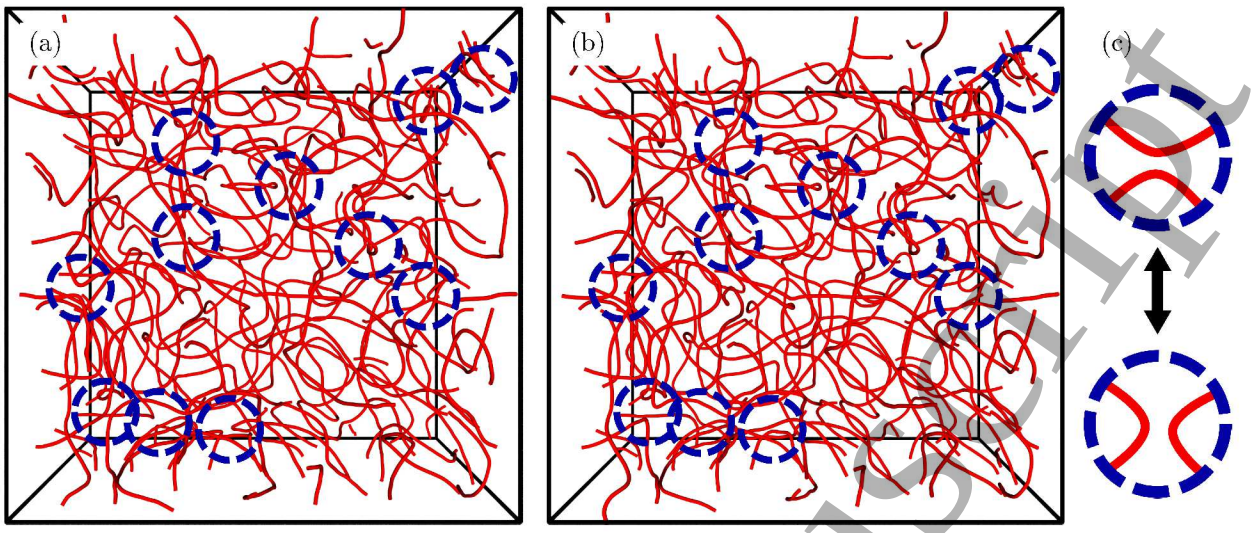


**Figure 4.** Nodal lines in slightly different arithmetic random waves (3-torus eigenfunctions) with energy $E = 236\pi^2$ ($N^2 = 59$). In (a), the amplitudes and phases or the 36 component plane waves are selected randomly. In (b) the eigenfunction is the same but with the phase of a single plane wave shifted by $\pi$. In most regions the local geometry of the nodal lines is barely affected by this change, but in several places (marked by blue circles) even this small adjustment induces a reconnection between vortex lines, changing the topology of the tangle. (c) illustrates how the vortices change locally during a reconnection; on the boundaries of the marked circle they remain essentially static, but in the centre they touch then split apart in a new configuration.

begin to show behaviour more complex than being simple puckered ellipses [28]. There should be no significant behaviour below the detectable lengthscales other than actual loop birth and death.

The expected rate for both reconnections and the birth/death of small loops has recently been derived for isotropic random wave systems by [30], and this result can be used to verify the numerical accuracy of our reconnection detection. The wavefunctions in [30] are given by superpositions of an infinite number of plane waves $a\exp(i(k\boldsymbol{n}\cdot\boldsymbol{r}+\omega t+\chi))$, with i.i.d Gaussian random amplitudes $a$, uniform random phase $\chi$, unit vectors $\boldsymbol{n}$ with uniform random orientation, $k$ values drawn from some wave power spectrum $P(k)$, and angular frequency $\omega$. In general for plane waves $\omega$ is a function of $k$, although in fact this is not necessary for the calculation. The rates of reconnections and birth/death in a given wavefield then depends on certain moments of the power spectrum, $\overline{k^2}, \overline{k^4}, \overline{\omega}, \overline{\omega^2}$:

$$\Omega_R = \frac{3}{10\pi^2}\sqrt{\frac{\overline{k^4}^3(\overline{\omega^2}-\overline{\omega}^2)}{\overline{k^2}(9\overline{k^4}-5\overline{k^2}^2)}} \tag{3}$$

$$\Omega_B = \Omega_D = \frac{1}{2}\Omega_R - \frac{1}{8\pi}\sqrt{\frac{\overline{k^2}^3}{3}(\overline{\omega^2}-\overline{\omega}^2)}\ , \tag{4}$$

where $\Omega_R, \Omega_B, \Omega_D$ are the rates of reconnections, loop birth, and loop death respectively.

These results can be applied to our monochromatic wavefield, but taking as the dispersion relation $\omega = ck$ all of the rates are naturally zero; the vortices are static even as the phase of the wavefield evolves around them. For the purposes of checking a reconnection rate using our algorithm, it is convenient to instead fix $\omega$ for each wave but allow its sign to vary, being

chosen randomly as positive or negative for each wave component. This is suggested in [30], where it is called the *monochromatic modulus* spectrum. Although not necessarily physical, this scheme is easily implemented numerically, and the combined rate of topological events should be $\Omega_R + \Omega_B + \Omega_D = (18 - 5\sqrt{3})k^3\omega/60\pi^2 \approx 3.91\lambda^{-3}s^{-1}$.

As with other random waves, this ensemble should be sufficiently well approximated by random waves with periodic boundaries (Section 2). We do so via 154 simulations of 3-torus eigenfunctions with $N^2 = 59$, in each case further evolving the phase of each plane wave component at a rate $\omega = \pm 1 s^{-1}$, incrementing in numerical steps $\Delta t = 7.5 \times 10^{-4} s$. This rate is chosen for numerical efficiency to balance the probability of multiple reconnections occurring in the same numerical step against the average number of steps between reconnections. Each eigenfunction is incremented by up to $\sim 785$ steps (total phase change $\omega\Delta t \sim 0.59$), during which changes in the number of vortices are detected as reconnections or loop births/deaths as described above. Although we do not distinguish here between reconnections and the birth/death of loops, the latter appears relatively uncommon, consistent with [30] in which its rate $\sim 26.5$ times lower than that of reconnection for the monochromatic modulus spectrum. Counting 17156 separate reconnection events over a total $\Delta t = 77.49 s$, the average combined rate of reconnections rate is $3.82\lambda^{-3}s^{-1}$. The discrepancy with the expected $3.91\lambda^{-3}s^{-1}$ is consistent with those in other quantities under periodic boundary conditions, especially as it is likely that our numerical method slightly undercounts the reconnection rate due to being unable to detect reconnections involving very small loops, where the length change is below a normal length change during evolution. It is also possible that the reconnection rate is suppressed by the same finite-size effects that slightly reduce the volume density of vortex lines. We therefore consider that this technique for detecting reconnections is numerically reliable.

We finally return to investigating whether the vortices involved in random reconnection events have length distributions that would fit the split-merge description of the Poisson-Dirichlet distribution. The primary concern here is that the reconnections counted should be genuinely independent events that are not biased by e.g. the time-periodicity of the monochromatic modulus spectrum, so we choose many different random initial conditions and evolve each only for long enough to detect a single reconnection, recording the lengths of the vortices involved. We also further simplify the spectrum to change only a single phase at the constant rate $\omega = 1 s^{-1}$, in which case with $\Delta t = \pi/100$, reconnections usually occur within 5 or increments. The reconnection frequency would not now match that of the monochromatic modulus spectrum, but our objective is now only to observe the length distribution of the vortices involved. Since our phase perturbations only need to be very small, and the configuration is not reused, we do not anticipate that the methodology should affect these statistics.

Figure 4 illustrates the instability of local vortex topology under this single phase perturbation, comparing two instances of similar eigenfunctions at $N^2 = 59$; the function of (b) is the same as (a) but with one of the 36 random phases shifted by $\pi$. Although the bulk of the vortex geometry is hardly changed, this small perturbation results in the 11 marked reconnection events, as well as others that cannot be seen as they have already occurred and reversed within the $0 \to \pi$ shift. In fact this example represents changing the phase of a relatively low-amplitude wave; in other cases it is possible to induce many more reconnections under the same $\pi$ phase shift.

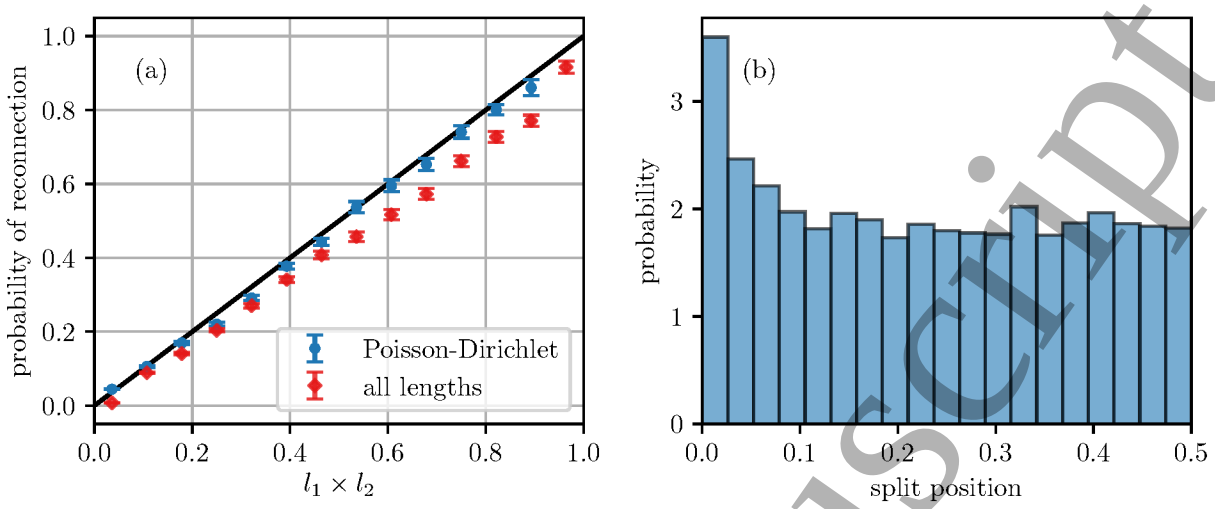


**Figure 5.** Statistics of arclength redistribution during splitting and merging of random wave vortices. (a) gives probabilities of reconnections between nodal lines of different lengths. In the x-axis, reconnection events are binned by the multiple $l_1 l_2$ of their length fractions $l_1$ and $l_2$; in the Poisson-Dirichlet model, this represents the probability of these lines being involved in the next reconnection event. The vertical axis counts the probability of these lines reconnecting (or a single line splitting) in the next reconnection event, found by taking a random wave under periodic boundary conditions and smoothly increasing the phase of a single plane wave component, stopping at the moment of the first reconnection as detected via the instantaneous jump in line length distribution. Assuming the reconnections obey the split-merge statistics of the Poisson-Dirichlet distribution, both axes should represent the same quantity and the distribution will be fit by a straight line with gradient 1. The blue points show these results for 15865 reconnections amongst lines in the Poisson-Dirichlet length regime ($l_1, l_2 \gg L^2\lambda$), where the statistics fit the expected straight line. The red points show the same results for 21574 reconnections including vortices of all lengths, but as expected do not fit to the split-merge prediction. (b) shows the statistics of the positions of reconnections that split vortex lines in the Poisson-Dirichlet regime. The horizontal axis marks the length fraction along the original line at which the next reconnection takes place, while the vertical axis shows the (normalised) relative frequency of these reconnections. The results come from 9515 independent vortex reconnection events at $N^2 = 59$, including only vortices whose initial lengths exceed 0.06 of the total vortex arclength in their eigenfunction.

The resulting statistics of vortex lengths during reconnection are summarised in Figure 5(a), for 22150 unrelated reconnection events from eigenfunctions with different random configurations. The dark points mark reconnection probabilities for lines in the PD regime only (here, length fraction $\geq$ 0.06 following the cutoff of Figure 2, although the result is robust to different choices). This includes 15259 of the 22150 detected reconnection events. The plot compares the multiple of the vortices' normalised lengths, $l_1 l_2$, with the numerically-recovered probability of their reconnection as compared against all the other possible reconnections for lines in the PD regime. If the split-merge procedure precisely describes the statistics of vortex reconnection, these quantities should be the same, and the results fit to a straight line with gradient 0.5. This result appears to match the behaviour of the vortex lines, and the split-merge process is a good descriptor of vortex reconnection rates in this regime. In contrast, the red points count all numerical reconnections, including those involving lines below the PD length regime. It is clear that the PD reconnection

statistics no longer apply, consistent with these lines being too short to interact uniformly with all others.

The split-merge process also requires that when a PD-regime line reconnects to split into two shorter lines, the vortex arclength should be distributed with uniform probability amongst the two new curves [9] (i.e. the reconnection is randomly positioned). The actual distribution of these length split fractions, recovered numerically from the simulations, is shown in Figure 5(b) for the 9515 independent vortex reconnection events in which a vortex line in the Poisson-Dirichlet regime undergoes a split. As expected, the split position appears uniform within statistical errors from the limited dataset, but only beyond the Poisson-Dirichlet length cutoff of $\sim 0.06\mathcal{L}$. Reconnections below this scale are more common, and represent small loops breaking off the Poisson-Dirichlet line, often with lengths even below even the fractal behaviour cutoff of $\sim 3.5\lambda$ (see Section 2). This may result from the smoothness of the wavefield limiting the random behaviour of the vortex lines on small scales, so that the formation of small loop-like structures is encouraged and the reconnections in this local region are relatively likely to germinate a new small loop. This deviation from the Poisson-Dirichlet split-merge statistics is to be expected when smaller loops are involved.

## 4. Discussion

We have demonstrated that the soup of filamentary vortex loops in wave chaos, sampled via large scale numerical simulations with periodic boundaries, falls into the universal scaling classes recently described by [13]. The vortex loops display all three anticipated length regimes; short-scale statistics that are not universal and depend on the local geometry of the wavefield, a power law scaling of vortex lengths at lengthscales larger than the wavefield decorrelation, and an eventual change to Poisson-Dirichlet statistics when the vortex loops become larger than the side length of the periodic cell. These results are 3D analogues to the well-studied percolation-like statistics of nodal domains in 2D quantum chaos. Importantly, they capture the effect of dimensionality on the vortex behaviour, as the wave vortices can now wind around one another in three dimensions. This result explains previous numerical observations of random wave vortices [4, 10], in which a deviation of the vortex tangle from ideal loop soup statistics was observed but not related directly to the impact of the periodic boundaries [4, 10]. The long vortex lines with non-trivial homology, which also arise generically in other classes of random filaments [2], are seen to arise naturally from the periodic boundaries. Although they can be considered as a type of boundary effect, they would always be present regardless of the periodic side length, with their contribution to the total vortex arclength balanced by the increased number of smaller, closed loop vortices. The length distribution of these long lines can be understood in terms of a statistical split-merge process, and by observing the changes in vortex lengths under perturbations to the configuration (or equivalently, under time evolution in non-monochromatic spectra) we have shown that this statistical process directly describes how vortices reconnect with one another under evolution processes. Although our analysis has focused on the monochromatic spectrum, such as would describe the chaotic eigenfunctions of 3D ergodic cavities, the same scaling results should apply to any isotropic spectrum even where this changes the local statistics dramatically.

The different statistical regimes of fractal loop soup behaviour can be understood in terms of a correction to the random reconnection statistics of an infinite random tangle, as a result of the

periodic boundaries. This description is summarised as follows: the most important property of the vortex lines is that beyond some small correlation lengthscale they behave as closed Brownian random walks (although they are self-avoiding according to local correlation functions, the isotropic soup of other lines in all directions means that their large scale directionality is not biased [2]). In the absence of periodic boundaries, this fixes their loop soup behaviour for all lengthscales above the small scale cutoff, so that all vortices form closed loops, and arbitrarily large loops can occur but only with low relative probabilities. Under perturbations to the state, or time evolution in polychromatic wavefields, the vortices will move and undergo reconnection events, but these are uniformly distributed about the tangle and the reconnections preserve the ideal loop soup distribution. The reconnections depend only on certain local statistics, and are not directly affected by periodicity, but the topology of the periodic cell changes the global statistics of how vortices approach one another, as long vortices can now wind throughout the periodic cell without necessarily being locally biased any more than in isotropic flat space. These highly extended vortices are long enough that they regularly pass close to other segments of themselves, as well as to almost all the other loops in a given cell, and the statistics of their reconnections are proportionately affected. The result is the ideal Poisson-Dirichlet distribution, in which the statistics of reconnections are simplified by the long loops filling the cell so uniformly that only their relative lengths contribute to the probability of their reconnecting.

It is interesting that despite the clearly delineated scaling regimes, the ideal loop soup power law scaling persists for loops with trivial homology even at lengthscales well into the Poisson-Dirichlet regime, with the Poisson-Dirichlet statistics made up instead by the NTH lines. Despite this clear separation of behaviours, the wrapping numbers of the NTH lines around the periodic boundaries (i.e. homology vectors) tend to be extremely small compared to the arclength of the entire line, such that the difference between NTH lines and closed loops would otherwise appear geometrically unimportant.

The reconnections are here considered only in a statistical sense, but previous work in the literature has established the local behaviour of the wavefield during such events; the vortices form hyperbolas, and at the moment of reconnection a critical point of the intensity (i.e. $\nabla|\psi|^2 = 0$) passes through the intersection point of the vortex strands [28, 31]. Analytically describing the statistics of these points remains an open problem [10], but it is tantalising that these numerical results, and recent work calculating reconnection rates [30], give specific bounds on how frequently their interaction with vortices becomes important. It is possible that our numerical techniques could be enhanced to capture the behaviour of these critical points and further refine the understanding of reconnection events. These phenomena also relate to other types of filamentary defects in complex 3D random waves; the intensity critical points sit on lines along which the vorticity $\frac{1}{2}\mathrm{Im}(\nabla\psi^* \times \nabla\psi)$ vanishes. These are more difficult to detect than vortex lines, as they lack a simple phase parameter whose accumulation can be detected, but they must wind through the field with their own random statistics [31]. These lines are unoriented, which is expected to change the parameter $\theta$ in (2) by affecting the way the lines can reconnect, and leading to different loop soup statistics within any Poisson-Dirichlet regime. Lines of this type also occur as e.g. the L lines in 3D polarisation fields [31], so it is important to note that the specific large scale behaviour of (oriented) vortices is not completely generic amongst other random filaments in similar fields.

Although reconnections instantaneously redistribute vortex arclength amongst the different vortices of the loop soup, they do not ultimately affect local geometrical statistics such as the average curvature and torsion of the curves. A different kind of measurement, sensitive to the large scale effects of these changes, is to ask instead about the topology of the vortex loops; whether they are knotted, or link with one another. It has been established that random waves at high energies generically contain knotted [11, 14] and linked [11, 25] vortices. These topological quantities measure the large scale entanglement of the loop soup, as they depend on the global winding of the loops about themselves on large scales, which may be quite decoupled from their local geometrical correlations. This topological sensitivity to large scale conditions has been seen in previous work where the statistics of vortex knotting vary significantly amongst different systems of random waves even at high energies where the local geometry is similar, due to the knot types feeling the effect of their boundary conditions [14]. It is possible that the right choice of topological quantity would reach a statistical steady state under reconnection processes, like the fractal and Poisson-Dirichlet regimes discussed above, but being instead a type of topological universality.

Although topological quantities are a natural choice for measuring the large scale entanglement of the system, it is not clear what measurements would be appropriate to quantify topological complexity. Properties of the knots and links can be captured using topological invariants, functions of the curve whose value depends only on its knot type, but these invariants are often abstract quantities without a simple physical interpretation [14], and their values may not be directly useful as descriptors of the vortex tangle as they can change significantly during a single reconnection between vortices. Attempts to quantify the topology of periodic systems would also be complicated by the NTH lines which, as they take advantage of the periodic boundaries, cannot be described as normal knots in $\mathbb{R}^3$ (where they are naturally represented as infinite periodically-repeating lines). These problems have been resolved in the literature for the certain measurements of linking between curves in periodic boundaries [32], but this method alone does not detect the knotting of a single curve, and still does not rule out large changes in the linking calculation as a result of even a single reconnection event. It is therefore an open question whether the vortex tangle will display topological universalities analogous to the scaling results discussed above, or whether different types of loop soups will exhibit characteristic differences in their knotting and linking despite their consistent large scale fractality.

## Acknowledgments

We are grateful to S G Whittington, R Evans, J H Hannay, and especially to M R Dennis, for useful discussions. This research was funded by the Leverhulme Trust Research Programme Grant No. RP2013-K-009, SPOCK: Scientific Properties of Complex Knots. This work was carried out using the computational facilities of the Advanced Computing Research Centre, University of Bristol.

## References

[1] T Vachaspati and A Vilenkin. Formation and evolution of cosmic strings. *Phys Rev D*, 30: 2036–45, 1984.

[2] M Hindmarsh and K Strobl. Statistical properties of strings. *Nucl Phys B*, 437:471–88, 1995.

[3] K Strobl and M Hindmarsh. Universality and critical phenomena in string defect statistics. *Phys Rev E*, 55:1120–49, 1997.

[4] K O'Holleran, M R Dennis, F Flossmann, and M J Padgett. Fractality of light's darkness. *Phys Rev Lett*, 100:053902, 2008.

[5] L D C Jaubert, M Haque, and R Moessner. Analysis of a fully packed loop model arising in a magnetic Coulomb phase. *Phys Rev Lett*, 107:177202, 2011.

[6] V Khemani, R Moessner, S A Parameswaran, and S L Sondhi. Bionic Coulomb phase on the pyrochlore lattice. *Phys Rev B*, 86:054411, 2012.

[7] R J Scherrer and J A Frieman. Cosmic strings as random walks. *Phys Rev D*, 33:3556–9, 1986.

[8] P-G de Gennes. *Scaling Concepts in Polymer Physics*. Cornell University Press, 1979.

[9] S Grosskinsky, A A Lovisolo, and D Ueltschi. Lattice permutations and Poisson-Dirichlet distribution of cycle lengths. *J Stat Phys*, 146:1105–21, 2012.

[10] A J Taylor and M R Dennis. Geometry and scaling of tangled vortex lines in three-dimensional random wave fields. *J Phys A*, 47:465101, 2014.

[11] A J Taylor. *Analysis of Quantised Vortex Tangle*. Springer Theses. Springer, 2017.

[12] A Nahum and J T Chalker. Universal statistics of vortex lines. *Phys Rev E*, 85:031141, 2012.

[13] A Nahum, J T Chalker, P Serna, M Ortuno, and A M Somoza. Length distributions in loop soups. *Phys Rev Lett*, 111:100601, 2013.

[14] A J Taylor and M R Dennis. Vortex knots in tangled quantum eigenfunctions. *Nat Comm*, 7:12346, 2016.

[15] M V Berry and M R Dennis. Phase singularities in isotropic random waves. *Proc Roy Soc Lond A*, 456:2059–79, 2000.

[16] M V Berry. Regular and irregular semiclassical wave functions. *J Phys A*, 10:2083–91, 1977.

[17] M Wright and R Weaver, editors. *New Directions in Linear Acoustics and Vibration*. Cambridge University Press, 2010.

[18] J W Goodman. Some fundamental properties of speckle. *J Opt Soc Am*, 66:1145–50, 1976.

[19] G Blum, S Dnutzmann, and U Smilansky. Nodal domain statistics: a criterion for quantum chaos. *Phys Rev Lett*, 88:114101, 2002.

[20] A G Monastra, U Smilansky, and S Gnutzmann. Avoided intersections of nodal lines. *J Phys A*, 36:1845–53, 2003.

[21] S Smirnov. Critical percolation in the plane: conformal invariance, Cardy's formula, scaling limits. *C R Acad Sci Paris*, 333:239–44, 2001.

[22] E Bogomolny and C Schmit. Percolation model for nodal domains of chaotic wave functions. *Phys Rev Lett*, 88:114102, 2002.

[23] J P Keating, J Marklof, and I G Williams. Nodal domain statistics for quantum chaotic maps. *New J Phys*, 10:083023, 2008.

[24] J P Keating, J Marklof, and I G Williams. Nodal domain statistics for quantum maps, percolation, and stochastic Loewner evolution. *Phys Rev Lett*, 97:034101, 2006.

[25] K O'Holleran, M R Dennis, and M J Padgett. Topology of light's darkness. *Phys Rev Lett*, 102:143902, 2009.

[26] Z Rudnick and I Wigman. On the volume of nodal sets for eigenfunctions of the laplacian on the torus. *Ann Henri Poincaré*, 9:109–30, 2008.

[27] M Krishnapur, P Kurlberg, and I Wigman. Nodal length fluctuations for arithmetic random waves. *Ann Math*, 177:699–737, 2013.

[28] M V Berry and M R Dennis. Topological events on wave dislocation lines: birth and death of loops, and reconnection. *J Phys A*, 40:65–74, 2006.

[29] A Nahum and J T Chalker. Phase transitions in three-dimensional loop models and the $cp^{n-1}$ sigma model. *Phys Rev B*, 88:134411, 2013.

[30] J H Hannay. Vortex reconnection rate, and loop birth rate, for a random wavefield. *J Phys A*, 50:165203, 2017.

[31] M R Dennis, K O'Holleran, and M J Padgett. The fractal shape of speckled darkness. *SPIE Proceedings*, 6905:69050C, 2008.

[32] E Panagiotou. The linking number in systems with periodic boundary conditions. *J Comp Phys*, 300:533–73, 2015.